HHS Public Access

Author manuscript

Adv Biol Regul. Author manuscript; available in PMC 2022 January 05.

Published in final edited form as:

Adv Biol Regul. 2021 January ; 79: 100781. doi:10.1016/j.jbior.2020.100781.

The Glo3 GAP crystal structure supports the molecular niche model for ArfGAPs in COPI coats

Boyang Xie[1], **Christian Jung**[1], **Mintu Chandra**[1], **Andrew Engel**[1], **Amy K. Kendall**[1,2], **Lauren P. Jackson**[1,2,3]

[1]Department of Biological Sciences, Vanderbilt University, Nashville, TN, USA

[2]Center for Structural Biology, Vanderbilt University, Nashville, TN, USA

[3]Department of Biochemistry, Vanderbilt University, Nashville, TN, USA

Abstract

Arf GTPase activating (ArfGAP) proteins are critical regulatory and effector proteins in membrane trafficking pathways. Budding yeast contain two ArfGAP proteins (Gcs1 and Glo3) implicated in COPI coat function at the Golgi, and yeast require Glo3 catalytic function for viability. A new X-ray crystal structure of the Glo3 GAP domain was determined at 2.1 Å resolution using molecular replacement methods. The structure reveals a Cys_4-family zinc finger motif with an invariant residue (R59) positioned to act as an "arginine finger" during catalysis. Comparisons among eukaryotic GAP domains show a key difference between ArfGAP1 and ArfGAP2/3 family members in the final helix located within the domain. Conservation at both the sequence and structural levels suggest the Glo3 GAP domain interacts with yeast Arf1 switch I and II regions to promote catalysis. Together, the structural data presented here provide additional evidence for placing Glo3 near Arf1 triads within membrane-assembled COPI coats and further support the molecular niche model for COPI coat regulation by ArfGAPs.

Introduction

Arf GTPase activating (ArfGAP) proteins comprise a family of regulatory and effector proteins defined by the presence of the ArfGAP domain (approximately 130-150 amino acids in length). ArfGAPs are found across eukaryotes: yeast contain five ArfGAPs, while mammalian cells contain over thirty[1]. ArfGAPs utilize their GAP domains to promote GTP hydrolysis on small GTPases in the Arf family[2-4]. Arf proteins are subclassified based on sequence homology and structural features.[3] Arfs undergo well-documented conformational

†Correspondence to lauren.p.jackson@vanderbilt.edu.

Credit Author Statement

BX, CJ, and AK performed protein expression and protein purification experiments. BX, AE, MC, and LPJ collected X-ray data and undertook structure determination and refinement. AE generated sequence alignments. BX and LPJ wrote the paper with input from all authors. LPJ conceived the project.

Conflict of interest

The authors declare no competing conflicts of interest.

changes in their switch I and switch II regions upon shifting nucleotide state[5,6] when a β hairpin between switch I and switch II allows communication from the protein N-terminus to the nucleotide binding site. In general, structural evidence suggests catalytic activity by GAP domains[7] relies on two key residues: an invariant “arginine finger” residue in the GAP and a conserved catalytic glutamine residue in its cognate GTPase. When GAP domains bind a GTPase, the GAP stabilizes the otherwise flexible switch II region, which in turn allows the catalytic glutamine residue to align a nucleophilic water molecule and promote hydrolysis[7].

There are eleven ArfGAP subfamilies[3], and members of two ArfGAP families specifically bind and regulate the small GTPase, Arf1. Arf1 plays critical roles in multiple membrane trafficking pathways mediated by vesicular coats, including a role in inducing membrane curvature[8]. On the Golgi apparatus, Arf1(GTP) recruits multiple coat protein complexes to promote and regulate vesicle formation[9]. Intrinsic GTP hydrolysis on Arf1 occurs slowly[10], so ArfGAPs are needed in cells to promote timely hydrolysis. ArfGAP proteins are critical regulators and effectors of COPI coat function. COPI[11-13] is essential for vesicular membrane trafficking in eukaryotes and has many established roles, including retrieval of endoplasmic reticulum (ER) proteins from the Golgi; ER/Golgi protein cycling; retrograde[14] and anterograde[15] trafficking within the Golgi stack; cargo recycling from endosomes to the TGN[16]; and organelle localization and cell shape[17]. Despite their cellular importance, the precise molecular role of ArfGAPs in regulating coats remains poorly understood. ArfGAPs are implicated in COPI coat assembly[18,19]; cargo/SNARE sorting[20-22]; and coat disassembly[23]. Budding yeast contain two essential ArfGAP proteins, Glo3 and Gcs1, which have overlapping functions[24]. Both yeast ArfGAPs have homologs/orthologs in mammalian cells: Gcs1 corresponds to ArfGAP1, while Glo3 corresponds to the ArfGAP2/3 family[1]. Yeast tolerate deletion of either the *GLO3* or *GCS1* genes individually but deletion of both is lethal[25].

Glo3 has been shown to play important roles in COPI coat assembly, including cargo selection and SNARE binding through its BoCCS (Binding of Coatomer, Cargo, and SNAREs) region[22]. Yeast require both a functional Glo3 GAP domain[22,26] and BoCCS region[22]. Recent data indicate yeast require Glo3 GAP activity,[19,26] because strains harboring the GAP-dead version of Glo3 (R59K) are not viable, even in the presence of Gcs1[26]. Biochemical data using yeast cell lysates[26] suggest only Glo3 stably associates with the COPI coat, although Gcs1 is also proposed to interact with COPI through a short hydrophobic motif[27]. Recent studies from the Briggs and Schwappach labs together proposed the “molecular niche” hypothesis: this suggests Gcs1 (ArfGAP1) and Glo3 (ArfGAP2/3) occupy different positions within assembled COPI coats[26,28]. Taken together, data indicate the ArfGAP1 and ArfGAP2/3 families may exhibit separation of function.

There are limited published structural data available on ArfGAP proteins that engage COPI coats. This work reports the first X-ray crystal structure of the yeast Glo3 GAP domain (residues 1-150). The structure reveals a Cys_4-type zinc finger motif and the position of the invariant arginine residues (R59) essential for function in budding yeast[26]. As expected, the Glo3 GAP domain exhibits sequence and structural similarity to other GAP domains in the ArfGAP family. However, comparison among available structures reveals ArfGAP2/3 family

members contain an extended helix α6 as compared to ArfGAP1 domains. Combining sequence and structural conservation with modeling suggests how Glo3 GAP likely engages Arf1(GTP) using a highly conserved interface. This new structure provides evidence for placement of the Glo3 GAP domain within assembled COPI coats on membranes and further supports the recently proposed molecular niche model[26].

Results

X-ray crystal structure of Glo3 GAP domain

We determined the structure of the *S. cerevisiae* Glo3 GAP domain (residues 1-150; Figure S1) to 2.1 Å resolution (Figure 1A; Table 1; Figure S1) using molecular replacement methods with human ArfGAP2 (PDB ID: 2P57; unpublished model) as an initial search model. Crystals belonged to space group $P2_1$ and contained four molecules in the asymmetric unit. All four copies show clear and well-ordered density from residues 8 to 145; additional density for residues 4-7 is visible in chain B only (representative experimental and final refined maps available in Figure S2). There is no significant difference between the four copies, and they overlay with an root mean square deviation (RMSD) value of 0.58 Å in CCP4 Superpose[29]. Following several rounds of iterative refinement in PHENIX[30,31], the final model demonstrated excellent overall geometry (Table 1) with 99% residues in Ramachandran favored regions and final R_{work}/R_{free} values of 0.191/0.247.

Overall, the Glo3 GAP domain (Figure 1A) is composed of a central core of five β-strands and six α-helices. Secondary structure prediction (PSIPRED[32]) successfully predicted all six helices but failed to predict the first three very short β-strands (β1, β2, β3). An additional short strand was predicted (not shown) following helix α6, which we were unable to visualize in the density. Strand β3 makes hydrogen bonding contacts with β4 and β5 to form the central three-stranded β sheet. The Glo3 GAP domain comprises a Cys_4 zinc finger containing the sequence C-XX-C-X_{16}-C-XX-C. The zinc finger is composed of three β strands (β1, β2, β4) together with adjoining loops and the N-terminal end of helix α2. The zinc ion is tetrahedrally coordinated by four conserved cysteine residues (Cys31, Cys34, Cys51, and Cys54), which each exhibit a distance between 2.3-2.5 Å from the zinc ion. The domain further contains a conserved arginine residue (R59) located in helix α2. This residue is predicted to act as an “arginine finger” during Arf1 catalysis[33], and comparison among GAP structures reveals it is well-positioned to play this role (see next section).

Comparison among ArfGAP domain structures

We compared the Glo3 GAP domain with thirteen ArfGAP domain structures deposited in the PDB using CCP4 Superpose[29] (Table 2) and ConSurf to evaluate conservation (Figure 2A); many of the available structures were deposited but remain unpublished. We first compared domains at the overall secondary structural level. Glo3 GAP is most similar to human ArfGAP2 (also called ZNF289; PDB ID: 2P57) and *P. falciparum* ArfGAP (PDB ID: 3SUB) based on overall RMSD (RMSD: 1.4 Å; Table 2). All thirteen structures align well in the region that comprises the first four helices (α1- α4) and β-strands (β1-4), while helices

α5 and α6 in the C-termini exhibit more variability. Globally, the Glo3 GAP looks similar to human GAP domains found in ArfGAP1, ArfGAP2, and ASAP3 (Figure 2B).

We further compared the highly conserved zinc finger core (Table 2) found in ArfGAP domains; this specifically includes three β-sheets (β1, β2, β4), adjoining loops, and the N-terminal end of helix α2. All ArfGAP domain zinc fingers align well with Glo3 GAP domain (RMSD: 0.5-1.4 Å; Table 2). As expected, the zinc finger is a conserved structural feature among ArfGAP proteins.[34,35] Furthermore, the invariant arginine residue (Glo3 R59) proposed to act as a catalytic "arginine finger" is conserved at the both the sequence (Figure S3A) and structural levels: this residue aligns very closely across multiple structures of GAP domains deposited in the PDB (Figure S3A). This residue has previously been reported to play either catalytic[36] or structural roles[34] (see Discussion) in different ArfGAP proteins.

However, there is one notable difference in the final helix located at the C-terminus of these GAP domains (Figure S3B). Helix α6 is especially different among ArfGAPs proteins. The GAP domains from multiple human ArfGAPs lack helix α6 altogether; examples include ASAP3 (PDBs: 2B0O, 3LVQ), SMAP1 (PDB: 2CRR), and ACAP1 (PDB: 3JUE). The human ArfGAP, Hrb (PDBa: 2D9L, 2OLM), contains an extremely short helix α6 with only a single turn. All of these ArfGAP domains are found in human proteins that lie outside the ArfGAP1 or ArfGAP2/3 families[35].

In addition, there appears to be a difference between the ArfGAP1 and ArfGAP2/3 family members. Two human ArfGAP1 crystal structures (PDBs: 3DWD, 3O47) reveal only four turns in helix α6. In contrast, helix α6 in the Glo3 GAP domain contains six turns and is thus longer (Figure S3B). Like Glo3, human ArfGAP2 (PDB ID: 2P57) and ArfGAP3 (PDB ID: 2CRW) each contain an extended helix α6. The ArfGAP3 structure (PDB: 2CRW) was determined using NMR, and it is clear from the data where helix α6 ends and leads into a region of high flexibility. The X-ray crystal structure of human ArfGAP2 is more ambiguous; there are clearly five turns in helix α6, and the last few residues suggest one more turn is possible. Overall, currently available GAP structures from different family members support the idea that ArfGAP2/3 proteins may differ at the C-terminus of the GAP domain, in addition to overall domain architecture. This has implications for COPI coat assembly (see Discussion).

Generation of yeast Glo3 GAP/Arf1 model

Controversy exists regarding how ArfGAP proteins engage Arf1[34,37]. This paper reports the first yeast GAP domain structure, but there are two relevant published mammalian X-ray structural models for Arf/ArfGAP interactions. The first is for murine ArfGAP1/Arf1[34] (PDB coordinates not available), and the second is for human ASAP3/Arf6[36] (PDB ID: 3LVQ). We note ArfGAP1 is the mammalian homologue of yeast Gcs1, which differs structurally and functionally from Glo3. Overall, the two models differ in where the GAP domain binds its Arf. Briefly, we combined conservation analysis in Consurf[38] with structural modeling in CCP4MG[39]. We propose the yeast Glo3 GAP/Arf1 interaction (Figure 3) likely resembles the ASAP3/Arf6 interaction, and this model has implications for assembly within the COPI coat on membranes (see Discussion; Figure 4).

The mouse ArfGAP1/Arf1 co-crystal X-ray structure[34] reveals ArfGAP1 binds Arf1 on a surface located away from the central zinc finger; in this model, coatomer was proposed to provide the arginine finger required for catalysis. Specifically, ArfGAP1 binds the Arf1 switch II region and helix α3, which are located on the opposite face from the zinc finger, and does not engage switch I. The Arf1 switch II interaction occurs via ArfGAP1 residues located on helices α3 and α6 (residues K68, I70, A116, E120, K122). This switch II interaction appears unlikely to happen with Glo3, because some residues are not conserved (K68, I70) while others have no equivalent.

The second part of the interaction requires both electrostatic and hydrophobic interactions between ArfGAP1 and Arf1 helix α3. The hydrophobic residues in ArfGAP1 (V54, H55, and F58) are conserved in Glo3 (V63, H64, F67; Figure S3A), but critical ArfGAP1 residues (R60, K68, and E71) that mediate salt bridge formation are not (Glo3 K69, T77, and N80). The ArfGAP1 lysine (K68) and glutamate (E71) residues are conserved among ArfGAP1 family members (not shown), which highlights a potential sequence and structural difference that delineates ArfGAP1 domains from the ArfGAP2/3 family and may have functional implications.

The structure of ASAP3 with Arf6 reveals a different mechanism[37]. In this model (Figure S4), ASAP3 uses its zinc finger to bind Arf6 switch I and II regions. ASAP3 GAP domain residues contributing to the buried interface are located on sheets β1 and β3, helices α2 and α4, and adjoining loops. The proposed arginine finger in ASAP3 is R469, which corresponds to Glo3 R59 in sequence alignments and structural superposition (data not shown). R469 protrudes into the active site, where it is positioned to act as an arginine finger to further stabilize the transition state and orient the nucleophile during catalysis. This ASAP3/Arf6 model[37] is similar to reported interactions between Ras and RasGAP proteins[33].

The Glo3 GAP/Arf1 interaction appears more likely to resemble the ASAP3/Arf6 interaction (Figure 3; Figure S4). The most highly conserved portion of Glo3 GAP across eukaryotes encompasses strands β3, β4, β5 and parts of helix α2. This region superposes well with the ASAP3 GAP domain (Figure 2B), indicating both sequence and structural conservation. Multiple ASAP3 residues required to interact with GTP-bound Arf6 switch I and II regions are conserved in the Glo3 GAP domain (residues Trp41, Ile52, Arg59, Val63, Leu73, Asp74; Figure 3B). We generated a yeast Arf1•AIFx model based on the Arf6•AIFx structure (3VLQ) using MODELLER[40]. This model superposes well (RMSD = 0.66 Å) with an X-ray structure of human GTP-bound Arf1 (PDB ID: 2J59), and Arf1 is highly conserved across eukaryotes (sequence identity= 77 %; sequence similarity= 96%), which gives confidence in this model for yeast Arf1(GTP). The model suggests key conserved Arf1 switch I (Thr45, Ile46, Pro47, Ile48) and switch II residues (Gln71, Asp72, Arg73) are positioned to interact with Glo3 (Figure 3B). The ASAP3 GAP domain was reported to promote hydrolysis on Arf1[37], lending further support to this model. Overall, we favor this model, but there are some caveats (see Discussion).

Discussion

Differences among ArfGAP proteins.

ArfGAP domains contain a C_4-type zinc finger motif and conserved arginine residue that may act as an “arginine finger” during catalysis. Based on structures for GAP domains that act on Ras and Rab GTPases[7], these structural features have been proposed to explain catalysis on Arf1. However, an X-ray structure of mammalian ArfGAP1 with Arf1[34] suggested the zinc finger played a structural rather than catalytic role. There are currently no structural data for yeast Gcs1, but there are multiple structures for the GAP domain in human ArfGAP1, which is thought to be functionally equivalent[1] to yeast Gcs1.

The Glo3 GAP structure presented here adds the first GAP structure for yeast ArfGAP domains and allows comparison among eukaryotic ArfGAP1 and ArfGAP2/3 family members. The conserved invariant arginine has now been visualized in multiple structures and appears to occupy the same position in GAP domains found in a variety of ArfGAPs (Figure S3A); data from yeast further suggest this is a catalytic arginine in Glo3[26]. Together, the Glo3 GAP domain structure and Arf1 modeling in this work further support a canonical role for this residue as the “arginine finger” required for catalysis. In contast, data from yeast suggest Gcs1 GAP activity is non-essential[26], and alignments reveal ArfGAP1 and ArfGAP2/3 family members have diverged in sequence immediately following the invariant arginine. Together, these data may further support the proposed structural role for this residue in the published mammalian ArfGAP1/Arf1 structure[34]. However, it should be noted this structure was determined in the presence of GDP (rather than GTP) and therefore depicts product rather than a transition state. Finally, there are conflicting data regarding whether or not COPI is required to promote catalysis by either ArfGAP1[34] or ArfGAP3[41] *in vitro*. It will be important to follow up with structural and biophysical studies in yeast.

Structural comparisons suggest there may be one difference in GAP domains from different families: ArfGAP1 family members appear to have a shorter helix α6 than do ArfGAP2/3 members (Figure S3B). The presence of this extended helix in Glo3 has important implications for where it can be accommodated in the membrane-assembled COPI coat (see below).

Model for Arf1 binding.

The zinc finger catalytic core and potential Arf1 binding residues are highly conserved in Glo3 GAP domain at both the sequence (Figure S3) and structural (Figure 2) levels, which supports the model for Arf1 binding proposed in Figure 3. However, there are caveats to this proposed model. First, the model was generated using human ASAP3 GAP, which exhibits some structural differences from Glo3 GAP. The Arf6 binding surface on ASAP3 (helix α2 and strand β5) is highly conserved with Glo3. The primary difference between the two domains is that ASAP3 GAP lacks helix α6. Second, the overall domain architecture for ASAP3 differs from Glo3. ASAP3 contains an ankyrin repeat domain following its GAP domain, and some residues within the ankyrin domain make minor interactions with Arf6. Glo3 does not contain an ankyrin domain, so there are no equivalent residues. Finally, ASAP3 contains a calcium binding site; the GAP domain uses two residues (Gln479/

Leu485) to coordinate a calcium ion. These residues are not conserved in Glo3 or other ArfGAP2/3 family members. Overall, despite these differences, the key residues and surface required for Arf binding are highly conserved between these two GAP proteins. Two additional pieces of data further support the model: ASAP3 was reported to promote catalysis on Arf1[36], and cryoET reconstructions[28] (next section) from reconstituted mammalian COPI show a similar binding mode.

Placement of Glo3 within membrane-assembled COPI coats.

The Glo3 GAP/Arf1 structural model presented in Figure 3 provides evidence for placement of Glo3 GAP within the COPI coat (Figure 4). Based on cryo-electron tomographic reconstructions from reconstituted coats, there are two proposed "types" of Arf1. The first (called γ-Arf1[26]) forms a triad with roughly three-fold symmetry[28,42] and is located adjacent to β'-COP and γ– COP subunits. The second (called β-Arf1) is located next to β-COP subunits; this interaction has been visualized using both X-ray crystallography[43] and cryo-electron tomography[42] (cryoET). The presence of these two Arfs is the basis for the "molecular niche" model, which proposes that Gcs1 binds β-Arf1 and Glo3 binds γ-Arf1[26]. This model places Gcs1 near δ-COP subunits, which is consistent with independent X-ray crystal data.[27]

The model presented here (Figure 4) supports cryoET reconstructions at low resolution placing human ArfGAP2 adjacent to γ-Arf1[28], since Glo3 is the yeast equivalent of mammalian ArfGAP2. Superposing the yeast Glo3 GAP/Arf1 model presented in Figure 3 onto γ-Arf1 located in triads reveals the Glo3 GAP domain could be accommodated at this position (one copy within the triad is shown in Figure 4). In contrast, modeling suggests the Glo3 GAP domain would experience clashes with the β-COP subunit while binding the β-Arf1 in multiple linkages (Figure S5); the GAP could only be accommodated at one observed linkage (linkage IV; Figure S6). In particular, the extended helix α6 in Glo3 appears to clash with β-COP (Figure S5A). Dodonova and colleagues reported the ArfGAP1/Arf1 interaction[34] could not be accommodated at the γ-Arf1 site in reconstituted COPI coats[28]. Together, current structural data from multiple groups support the molecular niche model, in which Glo3 (ArfGAP2/3 in humans) binds γ-Arf1. It remains to be confirmed structurally whether Gcs1 or ArfGAP1 specifically binds β-Arf1, and it will be important to test these structural hypotheses *in vitro* and *in vivo*.

Overall, in yeast, Glo3 appears to be the ArfGAP required for cell viability and function: GAP-dead Glo3 (R59K) cells cannot survive[26], while GAP-dead Gcs1 (R54K) cells are viable. The structural data presented here further support this invariant residue acting as the arginine finger required for catalysis. Data increasingly suggest Glo3 plays the more vital role in COPI coat function. One intepretation is that Glo3 is required to hydrolyze Arf1(GTP) to promote coat recycling, although Glo3 certainly has additional important functions[22]. The Glo3 GAP-dead mutant may "lock" assembled COPI coats onto membranes since Glo3 is known to stably associate with COPI[26], thereby preventing recycling of a coat that is essential for cellular function. Further structural studies on complexes will be required to understand molecular details of how Glo3 regulates coat assembly and function.

Materials and Methods.

Reagents.

Unless noted otherwise, all chemicals were purchased from Sigma (St. Louis, MO).

Cloning and plasmids.

An C-terminal GST-tagged fusion protein of Glo3 GAP domain (residues 1-150) was sub-cloned from full-length Glo3 into NdeI/BamHI sites of in-house vector pMWGST under control of a T7 promoter; this vector is a modified form of pMW172[44]. Full-length *S. cerevisiae* Glo3 was amplified by PCR from cDNA generated from the yeast genome kindly provided by the Graham lab (Vanderbilt University).

Protein expression and purification.

S. cerevisiae Glo3 GAP domain (residues 1-150) was expressed in and purified from BL21(DE3)pLysS cells (Invitrogen) for 16 to 20 hours at 22°C following induction with 0.4 mM Isopropyl β-D-1-thiogalactopyronoside (IPTG) at OD_{600} = 1.0. The protein was purified in buffer containing 10 mM HEPES (pH 7.5), 200 mM NaCl, 1 mM DTT with AEBSF protease inhibitor (Calbiochem) used at all stages of purification. Cells were lysed by a disruptor (Constant System Limited), and proteins were affinity purified using glutathione sepharose (GE Healthcare) in the purification buffer. The GST-tagged protein was cleaved overnight at 4°C by thrombin protease (Recothrom, The Medicine Company) and batch eluted. Eluted protein was further purified by gel filtration on a Superdex S200 Increase 10/300 GL column (GE Healthcare).

Crystallization and structure determination.

Purified yeast Glo3 GAP domain (residues 1-150) was concentrated to 5-10 mg/mL and crystallized in 2.0 M ammonium sulfate and 0.1 M sodium acetate pH 4.6 (Molecular Dimensions screen GCSG+ condition 35). Crystallization trays were set up using 400 nL drops on a Mosquito robot (LLP Lab Tech). Crystals were harvested directly from 96-well plates into 500 nL drops in reservoir buffer plus 25% glycerol for cryo-protection. Crystallographic datasets were collected at Argonne National Laboratory, sector LS-CAT, beamline 21-ID-D, from crystals flash frozen by plunging into liquid nitrogen. Data were collected at a wavelength of λ=1.77 Å. Crystals diffracted to 2.07 Å resolution and were of monoclinic space group $P2_1$ with unit cell dimensions a = 54.4 Å, b = 74.0 Å, c = 77.9 Å, α = 90.00°, β = 105.34°, γ = 90.00°. The data were integrated and merged in HKL2000[45] and further processed using the CCP4[46] and PHENIX[31] suites. The structure was phased using molecular replacement methods in Phaser[47] with the GAP domain from human ArfGAP2 as an initial model (PDB ID: 2P57). The Glo3 GAP model was first built using PHENIX AutoBuild[48]. Additional rounds of manual model building were undertaken in Coot[49] with iterative rounds of refinement using in PHENIX. Structure coordinates and maps have been deposited at the PDB (PDB ID: 7JTZ)

Sequence alignments.

In order to map conservation, GAP domain sequences from the ArfGAP1 and ArfGAP2/3 sub-families were aligned using Praline[50]. The following species were used in alignments: *S. cerevisiae, S. pombe, C. thermophilum, D. discoideum, C. elegans, A. thaliana, D. melanogaster, D. rerio, X. laevis, M. musculus*, and *H. sapiens*. A spreadsheet containing accession numbers for all genes used in the alignments is provided as Table 3.

Structural comparisons and visualization.

Superpose[29] in the CCP4 suite was used to compare structures of Glo3 GAP domain with other ArfGAP domains deposited in the PDB. The SSM algorithm was used to align the structures, and to determine RMSD and number of residues aligned between structures. The structure comparison was carried out on the complete GAP domain based on the overall secondary structure, as well as on the catalytic core (defined as Glo3 residues 27 – 65), which includes the zinc finger and arginine finger. All structural images or electron density maps presented in figures were generated using either the CCP4 Molecular Graphics (CCP4MG) program[39] or Coot[49].

Supplementary Material

Refer to Web version on PubMed Central for supplementary material.

Acknowledgements

BX, CJ, and AK performed protein expression and protein purification experiments. BX, AE, MC, and LPJ collected X-ray data and undertook structure determination and refinement. AE generated sequence alignments. BX and LPJ wrote the paper with input from all authors. LPJ conceived the project. BX, CJ, MC, AK, and LPJ are supported by NIH R35GM119525. LPJ is a Pew Scholar in the Biomedical Sciences, supported by the Pew Charitable Trusts. The authors declare no competing conflicts of interest.

References

1. Kahn RA et al. Consensus nomenclature for the human ArfGAP domain-containing proteins. J. Cell Biol 1, 1039–1044 (2008).
2. Cherfils J Arf GTPases and their effectors: assembling multivalent membrane-binding platforms. Curr Opin Struct Biol 29, 67–76 (2014). [PubMed: 25460270]
3. Jackson CL & Bouvet S Arfs at a glance. J Cell Sci 127, 4103–9 (2014). [PubMed: 25146395]
4. Gillingham AK & Munro S The small G proteins of the Arf family and their regulators. Ann Rev Cell Dev Biol 23, 579–611 (2007). [PubMed: 17506703]
5. Goldberg J Structural basis for activation of ARF GTPase: mechanisms of guanine nucleotide exchange and GTP-myristoyl switching. Cell 95, 237–48 (1998). [PubMed: 9790530]
6. Pasqualato S, Renault L & Cherfils J Arf, Arl, Arp and Sar proteins: a family of GTP-binding proteins with a structural device for 'front-back' communication. EMBO Rep 3, 1035–41 (2002). [PubMed: 12429613]
7. Vetter IR & Wittinghofer A The guanine nucleotide-binding switch in three dimensions. Science (80-.) 294, 1299–304 (2001).
8. Makowski SL, Kuna RS & Field SJ Induction of membrane curvature by proteins involved in Golgi trafficking. Adv. Biol. Regul 75, 100661 (2020). [PubMed: 31668661]
9. Donaldson J & Jackson C ARF family G proteins and their regulators: roles in membrane transport, development and disease. Nat Rev Mol Cell Biol 12, 362–375 (2012).

10. Kahn RA & Gilman AG The protein cofactor necessary for ADP-ribosylation of Gs by cholera toxin is itself a GTP binding protein. J Biol Chem 261, 7906–11 (1986). [PubMed: 3086320]
11. Duden R ER-to-Golgi transport: COP I and COP II function (Review). Mol Membr Biol 20, 197–207 (2003). [PubMed: 12893528]
12. Jackson LP Structure and mechanism of COPI vesicle biogenesis. Curr Opin Cell Biol 29C, 67–73 (2014).
13. Arakel EC & Schwappach B Formation of COPI-coated vesicles at a glance. J Cell Sci 131, (2018).
14. Popoff V, Adolf F, Brügger B & Wieland F COPI budding within the Golgi stack. Cold Spring Harb Perspect Biol 3, a005231 (2011). [PubMed: 21844168]
15. Yang J-S et al. COPI acts in both vesicular and tubular transport. Nat Cell Biol 13, 996–1003 (2011). [PubMed: 21725317]
16. Xu P et al. COPI mediates recycling of an exocytic SNARE by recognition of a ubiquitin sorting signal. Elife 6, (2017).
17. Desterke C & Gassama-Diagne A Protein-protein interaction analysis highlights the role of septins in membrane enclosed lumen and mRNA processing. Adv. Biol. Regul 73, 100635 (2019). [PubMed: 31420262]
18. Yang J-S et al. ARFGAP1 promotes the formation of COPI vesicles, suggesting function as a component of the coat. J Cell Biol 159, 69–78 (2002). [PubMed: 12379802]
19. Lewis SM, Poon PP, Singer RA, Johnston GC & Spang A The ArfGAP Glo3 Is Required for the Generation of COPI Vesicles. Mol Biol Cell 15, 4064–4072 (2004). [PubMed: 15254269]
20. Lee SY, Yang J-S, Hong W, Premont RT & Hsu VW ARFGAP1 plays a central role in coupling COPI cargo sorting with vesicle formation. J. Cell Biol 168, 281–90 (2005). [PubMed: 15657398]
21. Robinson M et al. The Gcs1 Arf-GAP Mediates Snc1,2 v-SNARE Retrieval to the Golgi in Yeast. Mol Biol Cell 17, 1845–1858 (2006). [PubMed: 16452633]
22. Schindler C et al. The GAP domain and the SNARE, coatomer and cargo interaction region of the ArfGAP2/3 Glo3 are sufficient for Glo3 function. Traffic 10, 1362–1375 (2009). [PubMed: 19602196]
23. Reinhard C, Schweikert M, Wieland FT & Nickel W Functional reconstitution of COPI coat assembly and disassembly using chemically defined components. Proc Natl Acad Sci U S A 100, 8253–8257 (2003). [PubMed: 12832619]
24. Poon PP et al. Retrograde transport from the yeast Golgi is mediated by two ARF GAP proteins with overlapping function. EMBO J 18, 555–564 (1999). [PubMed: 9927415]
25. Poon PP et al. Retrograde transport from the yeast Golgi is mediated by two ARF GAP proteins with overlapping function. EMBO J. 18, 555–564 (1999). [PubMed: 9927415]
26. Arakel EC et al. Dissection of GTPase activating proteins reveals functional asymmetry in the COPI coat. J Cell Sci (2019). doi:10.1242/jcs.232124
27. Suckling RJ et al. Structural basis for the binding of tryptophan-based motifs by δ-COP. Proc Natl Acad Sci U S A 112, 14242–7 (2015). [PubMed: 26578768]
28. Dodonova SO et al. 9Å structure of the COPI coat reveals that the Arf1 GTPase occupies two contrasting molecular environments. Elife 6, (2017).
29. Krissinel E & Henrick K Secondary-structure matching (SSM), a new tool for fast protein structure alignment in three dimensions. Acta Cryst D 60, 2256–68 (2004). [PubMed: 15572779]
30. Adams PD et al. PHENIX: a comprehensive, Python-based system for macromolecular structure solution. Acta Cryst D 66, 213–221 (2010). [PubMed: 20124702]
31. Liebschner D et al. Macromolecular structure determination using X-rays, neutrons and electrons: recent developments in Phenix. Acta Cryst D 75, 861–877 (2019).
32. Buchan DWA & Jones DT The PSIPRED Protein Analysis Workbench: 20 years on. Nucleic Acids Res. 47, W402–W407 (2019). [PubMed: 31251384]
33. Scheffzek K et al. The Ras-RasGAP complex: structural basis for GTPase activation and its loss in oncogenic Ras mutants. Science (80-.) 277, 333–8 (1997).
34. Goldberg J Structural and functional analysis of the ARF1-ARFGAP complex reveals a role for coatomer in GTP hydrolysis. Cell 96, 893–902 (1999). [PubMed: 10102276]

35. Kahn RA et al. Consensus nomenclature for the human ArfGAP domain-containing proteins. J Cell Biol 182, 1039–44 (2008). [PubMed: 18809720]
36. Ismail S. a, Vetter IR, Sot B & Wittinghofer A The structure of an Arf-ArfGAP complex reveals a Ca2+ regulatory mechanism. Cell 141, 812–21 (2010). [PubMed: 20510928]
37. Ismail SA, Vetter IR, Sot B & Wittinghofer A The Structure of an Arf-ArfGAP Complex Reveals a Ca2+ Regulatory Mechanism. Cell 141, 812–821 (2010). [PubMed: 20510928]
38. Ashkenazy H, Erez E, Martz E, Pupko T & Ben-Tal N ConSurf 2010: calculating evolutionary conservation in sequence and structure of proteins and nucleic acids. Nucleic Acids Res. 38, W529–W533 (2010). [PubMed: 20478830]
39. McNicholas S, Potterton E, Wilson KS & Noble MEM Presenting your structures: the CCP4mg molecular-graphics software. Acta Cryst D 67, 386–94 (2011). [PubMed: 21460457]
40. Webb B & Sali A Comparative Protein Structure Modeling Using MODELLER. Curr. Protoc. Bioinforma 54, 5.6.1–5.6.37 (2016).
41. Kliouchnikov L et al. Discrete determinants in ArfGAP2/3 conferring Golgi localization and regulation by the COPI coat. Mol Biol Cell 20, 859–69 (2009). [PubMed: 19109418]
42. Dodonova SO et al. A structure of the COPI coat and the role of coat proteins in membrane vesicle assembly. Science (80-.) 349, 195–8 (2015).
43. Yu X, Breitman M & Goldberg J A structure-based mechanism for Arf1-dependent recruitment of coatomer to membranes. Cell 148, 530–42 (2012). [PubMed: 22304919]
44. Owen DJ & Evans PR A structural explanation for the recognition of tyrosine-based endocytotic signals. Science (80-.) 282, 1327–32 (1998).
45. Otwinowski Z & Minor W Processing of X-ray Diffraction Data Collected in Oscillation Mode. Methods Enzym. 276, 307–326 (1997).
46. Winn MD et al. Overview of the CCP 4 suite and current developments. Acta Cryst D 67, 235–242 (2011). [PubMed: 21460441]
47. McCoy AJ et al. Phaser Crystallographic Software. J Appl Cryst 40, 658–674 (2007). [PubMed: 19461840]
48. Terwilliger TC et al. Iterative model building, structure refinement and density modification with the PHENIX AutoBuild wizard. Acta Crystallogr. Sect. D Biol. Crystallogr 64, 61–69 (2008). [PubMed: 18094468]
49. Emsley P, Lohkamp B, Scott WG & Cowtan K Features and development of Coot. Acta Crystallogr. D. Biol. Crystallogr 66, 486–501 (2010). [PubMed: 20383002]
50. Simossis VA & Heringa J PRALINE: a multiple sequence alignment toolbox that integrates homology-extended and secondary structure information. Nucleic Acids Res. 33, W289–W294 (2005). [PubMed: 15980472]

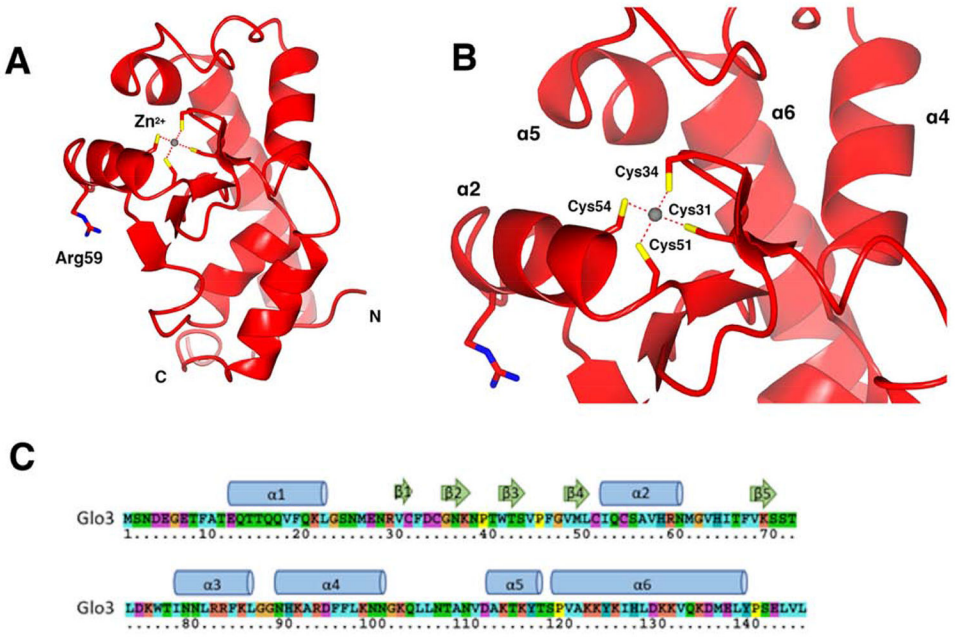

Figure 1. Glo3 GAP domain X-ray crystal structure.

(A) The Glo3 GAP domain (residues 1-150) X-ray crystal structure determined at 2.1 Å resolution is shown as a ribbon diagram with N- and C-termini, coordinated zinc ion (grey sphere), and conserved residues (Arg59, Cys residues as red cylinders) highlighted. (B) Close-up view of zinc finger: the conserved Arg59 side chain is shown as cylinders, and the location of the zinc ion (Zn^{2+}) within the zinc finger is shown as a grey sphere coordinated to four Cys residues. (C) The Glo3 GAP sequence marked with secondary structural elements. The GAP domain contains six α-helices and five β-strands.

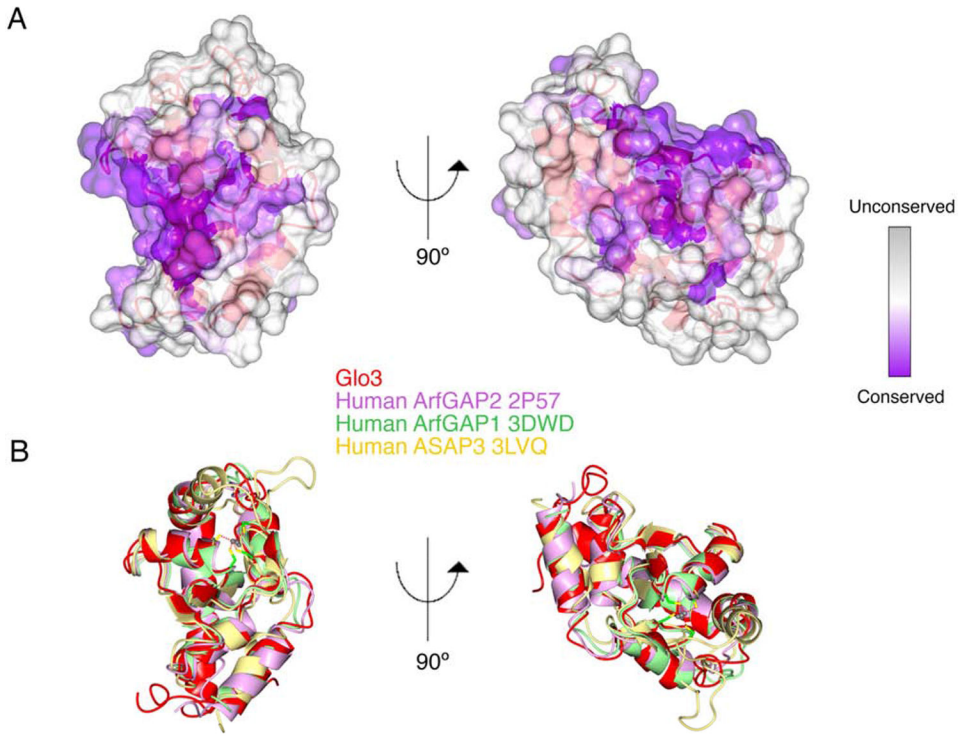

Figure 2. Glo3 GAP domain structural conservation.

(A) Two views (rotated 90 degrees) showing overall Glo3 GAP conservation mapped onto its X-ray crystal structure (shown as a surface). Grey areas denote no conservation, while purple represents identity. (B) Two views (rotated 90 degrees) showing overall structural conservation between yeast Glo3 GAP and three human ArfGAP domain structures (ArfGAP1, ArfGAP2, and ASAP3).

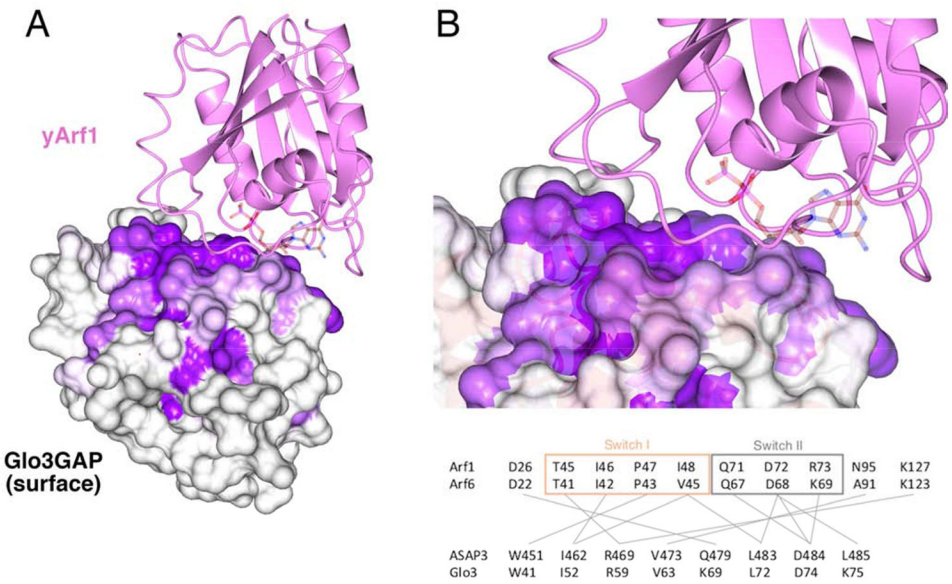

Figure 3. Model for yeast Glo3 GAP binding to Arf1.

(A) Model of Glo3 GAP/yeast Arf1 generated using ASAP3/Arf6 crystal structure as a model (PDB: 3LVQ; Figure S4). Yeast Arf1 (yArf1) is shown as pink ribbons and Glo3 GAP domain is shown as a surface colored by conservation. The predicted Arf1 binding interface (dark purple) is highly conserved in the Glo3 GAP domain, which supports a model resembling the ASAP3/Arf6 interaction. The nucleotide from 3LVQ is shown as transparent cylinders to denote its binding site. (B) Upper panel: Close-up view of Glo3 GAP/yArf1 model interface; the nucleotide from 3LVQ is shown as transparent cylinders to delineate the binding site. Lower panel: Residues in the proposed interaction interface are conserved, including key Arf switch I and II residues and the arginine finger in both GAP domains (Glo3 Arg59/ASAP3 Arg469). Grey lines represent proposed molecular interactions between Arf switch I/switch II residues and their counterparts on each GAP domain.

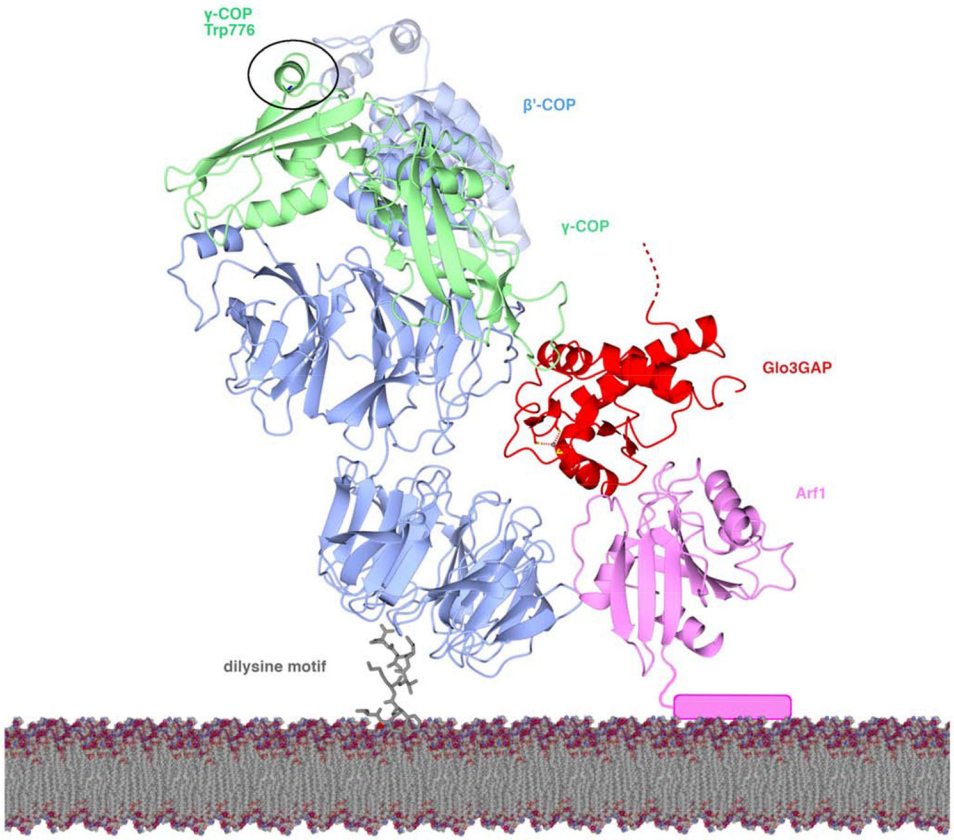

Figure 4. Model for Glo3 GAP domain within membrane-assembled COPI coats.

Model for the interaction of Glo3 GAP (red ribbons) with γ-Arf1 (pink ribbons with N-terminal amphipathic helix shown as cylinder). Two different Arf1 positions are proposed in COPI coats; this view represents one copy of γ-Arf1 within a triad (see text for details). This model shows Glo3 GAP acting on γ-Arf1, which is located in Arf1 triads found adjacent to β'-COP subunits (blue ribbons; WD-repeat domains and solenoid). The γ-COP appendage domain (green ribbons) is also shown. This model was generated by combining the Glo3 GAP/yArf1 model presented in Figure 3 with cryoET reconstructions (PDB ID: 5NZS) of reconstituted COPI coats. The Glo3 BoCCS region begins at the red dashed/dotted line. The precise molecular position of the Glo3 BoCCS and GRM regions are unknown, but the known Glo3 binding site on γ-COP appendage domain is marked as a black circle. (Figure S5 shows models for Glo3 GAP interacting with β-Arf1 positions at different linkages within the COPI coat.)

Table 1.
Glo3 GAP crystallographic data collection and refinement statistics.

Values in parentheses refer to the highest resolution shell.

Data Collection Statistics		
Beamline	LSCAT-21IDD	
Space group	$P2_1$	
Wavelength (Å)	1.77	
a, b, c (Å)	54.4, 74.0, 77.9	
α, β, γ (degrees)	90.0, 105.3, 90.0	
Resolution range (Å)	41.20 - 2.07	
R_{merge}	0.07785 (2.039)	
Mean $I/\sigma I$	13.1 (0.80)	
Completeness (%)	92.6	
Multiplicity	2.0	
CC1/2	0.876 (0.00377)	
Total reflections	66787 (6852)	
Unique reflections	34077 (3495)	
Refinement		
Resolution Range (Å)	41.20 - 2.07	
No. reflections	34077	
R_{work}/ R_{free}	0.191/0.247	
Number of atoms	Protein	4458
	Ligands (glycerol, zinc)	16
	Solvent (water molecules)	51
	Wilson B-factor (Å^2)	37.47
R.M.S.D. from ideal values	Bond lengths (Å)	0.007
	Bond angles (°)	0.89
Ramachandran plot	Favored region (%)	99.3
	Allowed (%)	0.7
	Outliers (%)	0
	Rotamer outliers (%)	0.80
	Average B-factor (Å^2)	50.92
PDB ID	7JTZ	

Table 2.
Structural conservation among ArfGAP proteins.

Glo3 GAP domain was compared with thirteen structures deposited in the PDB. The whole GAP domain and zinc finger core were compared using CCP4 Superpose. Root mean square deviation (r.m.s.d.) values are reported in angstroms.

PDB ID	Protein(s)	Species	Overall r.m.s.d. (A)	Zinc finger "core" r.m.s.d. (A)
2P57	ArfGAP2	*Homo sapiens*	1.39	0.56
3SUB	ArfGAP	*Plasmodium falciparum*	1.4	0.52
3DWD	ArfGAP1	*Homo sapiens*	1.51	0.57
2CRR	SMAP1	*Homo sapiens*	1.74	0.76
2OLM	RIP/HRB	*Homo sapiens*	1.75	1.32
2B0O	ASAP3	*Homo sapiens*	1.77	0.53
3LVQ	ASAP3/Arf6	*homo sapiens*	1.77	0.62
2CRW	ArfGAP3	*Homo sapiens*	1.86	0.91
3O47	ArfGAP1/Arf1	*Homo sapiens*	1.86	0.64
2OWA	ArfGAP	*Cryptosporidium parvum*	1.88	0.66
3JUE	ACAP1	*Homo sapiens*	2.16	0.58
2D9L	RIP/HRB	*Homo sapiens*	2.2	1.46
3T9K	ACAP1/integrin β1	*Homo sapiens*	2.24	0.76

Adv Biol Regul. Author manuscript; available in PMC 2022 January 05.

Table 3.

Sequences used in alignments.

Gene name	Gene ID	Accession #	ArfGAP family	Species	Isoform	Notes
ADP ribosylation factor GTPase activating protein 1	55738	XP_011527203	ArfGAP1	H_Sapiens	X1	
ADP-ribosylation factor GTPase activating protein 1	228998	XP_036017629	ArfGAP1	M_musculus	X2	
ADP ribosylation factor GTPase activating protein 1 S homeolog	447049	XP_018093019.1	ArfGAP1	X_laevis	X1	
ADP-ribosylation factor GTPase activating protein 1	100149572	NP_001007304	ArfGAP1	D_rerio		
ADP-ribosylation factor GTPase activating protein 1	39417	NP_524040	ArfGAP1	D_melanogaster		
Arf-GAP domain-containing protein	172643	NP_492310	ArfGAP1	C_elegans		BLAST identified only 1 homolog
ARF-GAP domain 7	818331	NP_001031503.1	ArfGAP1	A_thaliana		
Arf GTPase activating protein	8623152	XP_640542.1	ArfGAP1	D_discoideum		BLAST identified only 1 homolog
ARF GTPase activator-like protein [Chaetomium thermophilum var. thermophilum DSM 1495]	18257920	XP_006694297.1	ArfGAP1	C_thermophilum		
glo3 putative ARF GTPase-activating protein	2541825	NP_594843.2	ArfGAP1	S_pombe		
GCS1 GTPase-activating protein GCS1 [*Saccharomyces cerevisiae S288C*]	851372	GFP63814.1	ArfGAP1	S_cerevisiae		
ADP ribosylation factor GTPase activating protein 2	84364	Q8N6H7.1	ArfGAP2/3	H_Sapiens		
ADP ribosylation factor GTPase activating protein 3	26286	NP_055385.3	ArfGAP2/3	H_Sapiens		
ADP-ribosylation factor GTPase activating protein 2	77038	NP_076343.2	ArfGAP2/3	M_musculus	2	
ADP ribosylation factor GTPase activating protein 2 L homeolog	108713765	XP_018112824.1	ArfGAP2/3	X_laevis	X2	
ADP-ribosylation factor GTPase activating protein 2	641490	NP_001032507.1	ArfGAP2/3	D_rerio		
ArfGAP3 ADP-ribosylation factor GTPase activating protein 3	40487	NP_001262216.1	ArfGAP2/3	D_melanogaster	E	
Arf-GAP domain-containing protein	172643	NP_492310.1	ArfGAP2/3	C_elegans		Blast identified only 1 homolog
ARF-GAP domain 9	834718	NP_199487.1	ArfGAP2/3	A_thaliana		
Arf GTPase activating protein	8623152	XP_640542.1	ArfGAP2/3	D_discoideum		Blast identified only 1 homolog
ARF GTPase activator-like protein	8257920	XP_006694297.1	ArfGAP2/3	C_thermophilum		
Putative ARF GTPase-activating protein	2541825	NP_594843.2	ArfGAP2/3	S_pombe		
GLO3 ADP-ribosylation factor GTPase-activating protein	856859	NP_011048.1	ArfGAP2/3	S_cerevisiae		